International Journal of Civil Engineering

Structure
Earthquake

Improved seismic design of structural frames by optimization of equivalent lateral load pattern

M. Shahrouzi[1,*], A.A. Rahemi[1]

Received: October 2012, Revised: August 2013, Accepted: January 2014

Abstract

Well-known seismic design codes have offered an alternative equivalent static procedure for practical purposes instead of verifying design trials with complicated step-y-step dynamic analyses. Such a pattern of base-shear distribution over the building height will enforce its special stiffness and strength distribution which is not necessarily best suited for seismic design. The present study, utilizes a hybrid optimization procedure to seek for the best stiffness distribution in moment-resistant building frames. Both continuous loading pattern and discrete sizing variables are treated as optimization design variables. The continuous part is sampled by Harmony Search algorithm while a variant of Ant Colony Optimization is utilized for the discrete part. Further search intensification is provided by Branch and Bound technique. In order to verify the design candidates, static, modal and time-history analyses are applied regarding the code-specific design spectra. Treating a number of building moment-frame examples, such a hyper optimization resulted in new lateral loading patterns different from that used in common code practice. It was verified that designing the moment frames due to the proposed loading pattern can result in more uniform storey drifts. In addition, locations of the first failure of columns were transmitted to the upper/less-critical stories of the frame. This achievement is important to avoid progressive collapse under earthquake excitation.

Keywords: *Seismic design, Structural optimization, Failure sequence, Building moment frame.*

1. Introduction

Seismic design is a challenging task since its loading is primarily a kind of ground acceleration rather than pure lateral forces. In order to simplify the design procedure the well-known codes of practice have offered application of equivalent static forces as height-wise distribution of the design base-shear [1, 2]. However, it is only a simplified design procedure rather than an exact analysis.

Recent investigations have proved that the current code-based equivalent static lateral load procedure may not essentially result in proper seismic behavior of the structure. Hosseini and Motamedi used non-linear analysis of some reinforced concrete buildings and observed that true distribution of base-shear over the frame's height is not exactly the same as that predicted by the design codes [3]. Moghaddam and Hajrasouliha employed the optimality criteria method for lumped mass model of the building to optimize ductility ratios over the stories of such a model [4]. As a result the conforming storey shears and loads were different from those recommended by conventional code practice. Consequently, they offered a theory that implies the desired seismic behavior will be achieved in case of uniform distribution of the drift response among the building stories [4,5]. Kaveh et al verified that optimal plastic hinge locations in a structural frame are dependent to its design [6]. Shahrouzi and Rahemi considered sizing design of steel structures under various lateral loading patterns and showed that the code-based design is neither optimal nor can prevent plastic hinges from arising at the lower stories of the building [7]. As such lower storey columns play critical role in the structural stability; their failure can cause consequent progressive collapse of the entire frame.

In the other hand, lateral loads derived from height-wise distribution of the base-shear depend on the existing distribution of stiffness in the building design and vice versa. Hence, any pattern of equivalent lateral design loads enforces its correspondent seismic behavior and failure sequence in the building.

The present work concerns variation of resulting storey shear and loading pattern with sizing variation of the frame members and seeks the best pattern via optimization. The developed hyper optimization algorithm is more complicated than pure sizing because it consists of searching both the continuous lateral load factors and the discrete member sizing variables, simultaneously. As a result, novel patterns of base-shear distribution in the form of lateral design loads are obtained treating a number of examples. The new designs are then compared with those based on code-recommended loading pattern considering the structural response and column failure sequence.

** Corresponding author: shahruzi@khu.ac.ir*
1 Faculty of Engineering, Kharazmi University, Tehran, Iran

[Downloaded from ijce.iust.ac.ir on 2026-09-14]

2. Base-Shear Distribution in Modal Analysis and Equivalent Static Design Procedure

According to different response characteristics under various earthquake excitations, the seismic design codes have offered a set of smooth design spectra based on rigorous statistical analyses as a unique source of loading. The design procedure consists of trial and error when controlling the modal responses due to the standard earthquake spectra with their acceptable limits. The base-shear for such a spectral analysis is then distributed over the building height according to the following basic relation:

$$F_{ij} = \frac{m_i \varphi_{ij}}{\sum_{k=1}^{N} m_k \varphi_{kj}} V_j \quad (1)$$

In which φ_{ij} stands for the j[th] modal shape at the i[th] storey (degree of freedom) with the mass m_i while V_j represents the base-shear in the j[th] mode for which, the corresponding lateral force at every i[th] storey is denoted by F_{ij}. N is the total number of stories in such a shear-building model.

In order to reduce the trial and error in spectral design to a straight forward procedure, the seismic codes have accepted using the simplified static loading procedure which is, somehow, equivalent to employ only one artificial vibration mode. Its mode shape is evaluated at every storey with the height h_i as:

$$\varphi_i = \frac{h_i}{\sum_{k=1}^{N} h_k} \quad (2)$$

This way, the seismic design is dictated to the structure using the corresponding distribution of the code-specific base-shear V determined for seismicity of the site and behavior factor of the lateral load resistant system:

$$F_i = \frac{m_i h_i}{\sum_{k=1}^{N} m_k h_k} V \quad (3)$$

However, as a single modification an additional force at the roof storey is exerted to this artificial lateral load pattern in case of high-rise buildings [2].

3. Problem Formulation for Optimization of Lateral Load Pattern and Structural Sizing

According to the described relations it is evident that modal lateral forces are dependent to distribution of strength and stiffness in the structure. The equivalent static procedure dictates such a distribution to the design while it is not necessarily the best. The most appropriate seismic design should be searched via optimization framework.

In the sizing optimization; various combinations of cross sections are assignable to the structural members; that means a dramatically large search space for common problems.

For example, consider a moment frame with 15 member groups when there are only 10 cross sections available to select for each group. The total number of possible design alternatives will then be 10^{15} which is quite large. However, just a fraction of such a search space will be considered feasible due to the design code requirements. The section indices assignable for member groups are considered the sizing design variables in the problem formulation that forms a combinatorial type of optimization.

Feasibility and optimality of every structural model in the sizing search space is dependent to its loading including the exerted lateral forces in the equivalent static design procedure. Hence, determining the suitable pattern of base-shear distribution is a complicated hyper optimization problem in which the primary design variables are the storey load distribution coefficients, y_i, while the secondary variables are the sizing indices, s_i. The corresponding lateral forces F_i are then be distributed using the following relation:

$$F_i = \frac{y_i}{\sum_{k=1}^{N} y_k} V \quad (4)$$

where V is the code-specific base-shear. Here, any design vector $\underline{X}$ includes both the corresponding variables y_i and s_i to enable simultaneous optimization of the base-shear distribution pattern and frame sizing, respectively.

$$\underline{X} = \{y_1, ..., y_N, s_1, .., s_M\} \quad (5)$$

During the meta-heuristic search, various design vectors are sampled among the search space and their feasibility and desirability is determined via evaluation of the fitness function. Then the fittest feasible individual vector achieved over iterations of the employed algorithm is announced as the optimal design.

The problem formulation for such a hyper optimization is given as:

Maximize

$$Fitness(\underline{X}) = -w(\underline{X})(1 + \sum_{l} K_P C_l + K_R C_R) \quad (6)$$

Subject to:

$$g_1 = \frac{D_i}{D_{allowable}} - 1 \le 0 \quad (7)$$

[Downloaded from ijce.iust.ac.ir on 2026-09-14]

$$g_2 = \begin{cases} \frac{f_a}{F_a} + \frac{f_b}{F_b} - 1 \le 0 & if \quad \frac{f_a}{F_a} \le 0.15 \\ \frac{f_a}{0.6F_y} + \frac{f_b}{F_b} - 1 \le 0 & otherwise \end{cases} \tag{8}$$

$$g_3 = \frac{f_a}{F_a} + \frac{c_m f_b}{(1 - f_a / F_e) F_b} - 1 \le 0 \tag{9}$$

$$g_4 = \frac{f_s}{F_s} - 1 \le 0 \tag{10}$$

$$C_l = \begin{cases} \sum_j g_l{}^j & if \quad g_l{}^j > 0 \\ 0 & otherwise \end{cases} \tag{11}$$

for:

$i = 1,..., N$, $j = 1,..., NumElements$,

$l = 1,..., NumConstraints$

$w(\underline{X})$ is the total structural weight while code-specific stress and displacement constraint violations during dynamic analysis are considered in C_l. K_P denotes the corresponding penalty coefficient. C_l is taken zero for any non-violated constraint otherwise it represents the amount of the l^{th}-constraint violation. $D_{Allowable}$ and D_i denote the allowable and resulting drift in the i^{th} storey, respectively. For every j^{th} element, f_a, f_b, f_s are the resulting axial, bending and shear stresses, respectively. F_a, F_b, F_s as the corresponding allowable stress values and the factors F_e, c_m are determined due to the design code regulations [8].

The additional term $K_R C_R$ of the fitness relation in the present work is considered to remunerate a structural safety measure based on which storey be the first for column plastic hinge occurrence. K_R is a remuneration coefficient and C_R is evaluated as:

$$C_R = \frac{\sum_{i=1}^{n} \left| (e^{\lambda B(i)/N} - e^{\lambda J(i)/N}) \right|}{\sum_{i=1}^{n} \left| (e^{\lambda B(i)/N} - e^{\lambda Q(i)/N}) \right|} \tag{12}$$

Whereas i counts for the building storey number; $B(i)$ and $Q(i)$ form the best and the worst arrange of stories for plastic hinge occurrence, respectively. The frame stories are numbered from lower (as 1) to the uppermost level (N). Therefore, with $\underline{B} = < N, N-1,...,1 >$ the best desired arrange will correspond occurrence of plastic hinge from upper stories to lower ones and vice versa for the worst arrange $\underline{Q} = < 1,2,..., N >$. $J(i)$ denotes the arrange resulted by analysis of any current model corresponding to its $\underline{X}$ vector. Here-in-after, the formula constants: n and λ are taken 5 and 3, respectively.

Since the computational cost required in extensive sampling the large search space by meta-heuristic methods is quite high, it is worth using linear analyses to evaluate the fitness function. Note that the structure behaves linearly up to the first plastic hinge formation at the maximum stress point. Thus the first hinge location can be evaluated by the maximum combined stress ratios even by a linear spectral analysis. The required spectral dynamic and static analysis cores are programmed and merged with in the developed optimization modules in the present work.

4. Utilized Optimization Framework

The primary design variables, y_i, continuously vary in domain (0,1] and thus form a design space with infinite number of points. The *harmony search*, HS algorithm is suited for this stage because of its capability to assess continuous search spaces [9-13].

First introduced by Geem et. al. [9], the HS terminology is based on simulating the process musician brain employs to improvise a new music or set of notes considering its best previous experiences in their current memory. A degree of free exploration for other pitches is also implemented in such a process. Therefore, memory consideration, pitch adjustment and random exploration are mixed with fitness-based selection as major rules of HS. For an optimization with a typical design variable *Y*, harmony search algorithm can be presented via the following steps:

1) Set the algorithm control parameters: harmony memory size, HMS, being the number of vectors in the memory; harmony memory consideration rate, HMCR; pitch adjustment rate, PAR; bandwidth, BW and maximum number of iterations, NI_{HM}.

2) Initiate the first population of vectors in the harmony memory, HM, with random numbers in their allowable range. Then evaluate fitness of all HM vectors.

3) Generate a candidate solution vector, $\underline{Y}'$. With the probability, *1-HMCR*, randomly initiate all components of $\underline{Y}'$; otherwise:

- select $\underline{Y}'$ as an entire vector randomly from those stored in the current HM.

- for each components of $\underline{Y}'$, with the probability PAR alter the corresponding value (design variable) according to the relation:

$$Y'_j = \min(\max(Y'_j \pm rand * BW, Y_j^{LowerLimit}), Y_j^{UpperLimit}) \tag{13}$$

rand is a uniformly generated continuous random number between 0 and 1.

4) Update the HM: Replace $\underline{Y}'$ with the least fit $\underline{Y}$ in the current HM if $\underline{Y}'$ is fitter than it

In this study, the vector $\underline{Y}$ forms the first part of total design vector $\underline{X}$ which corresponds to load pattern distribution factors, y_i in Equation 5.

[Downloaded from ijce.iust.ac.ir on 2026-09-14]

The second part of $\underline{X}$ is designed to search a discrete space of possible combinations altering profile sizing indices, s_i. Using integer indices is preferred because it not only reduces a continuous space to a limited discrete one, but also several structural properties of any cross section are addressed only by one index. Altering the section index may increase one property and increase another, so it is not logical to take a section property itself as a design variable for an integrated structural analysis.

In *memetic algorithms* fitness evaluation of an individual is delayed to completion of its further *local search* or *educational growth* [14].The method developed in this research uses similar approach since for every candidate load-pattern generated during the first part of optimization as $\underline{Y}$ sub-vector, the frame member's sizing in the second part; i.e. the $\underline{S}$ vector of section indices, is also optimized so that the entire design vector $\underline{X}$ is completed and its fitness can be evaluated.

The main meta-heuristic algorithm is based on sampling the search space individuals by forming their entire design vector $\underline{X} = \{y_1,..., y_N, s_1.., s_N\}$. Such a framework for simultaneous optimization of lateral load pattern and frame sizing is crucial for true decision making and seeking the loading patterns that correspond to the best distribution of structures' stiffness and strength resulting in its desired seismic response.

Ant colony optimization, ACO, stands for a class of algorithms mainly inspired by indirect information sharing process of real ants in the nature [15]. It has already shown outstanding efficiency and rapid convergence rate in several discrete problems [16].

Hence in the present study, a Min-Max variant of ACO is utilized for the second part of the hyper-optimization where rapid discrete search is needed to perform sizing as soon as every load pattern is sampled from its infinite continuous search space.

ACO requires a characteristic graph to deposit pheromone values on its edges. An edge is defined between two adjacent graph vertices. Such a characteristic bi-partite graph is already introduced for structural sizing problems as a bi-partite graph [17]. Assigning a section index to a member-group is analogous to drawing an edge between the corresponding member-group vertex in the 1st part of the graph and the other vertex in the 2nd part denoting the assigned section index. In the proposed sizing optimization, the amount of pheromone deposit on every such edge is thus taken as:

$$\Delta\tau = \frac{W^{\max}}{L^{Best}} \tag{14}$$

where $W^{\max}$ is the heaviest possible structural weight using available section-list. L^{Best} is assigned $L^{IterationBest}$ or $L^{GlobalBest}$ alternatively every other time that an artificial tour is constructed. $L^{IterationBest}$ is taken analogous to the best structural weight found in the current iteration of the search while $L^{GlobalBest}$ denotes the best-so-far solution found over all previous iterations up to the current. Consequently, the new amount of pheromone at any edge from node-i to node-j after deposition and evaporation is computed as:

$$\tau_{ij}^{k+1} = (1-\rho)\tau_{ij}^{k} + \Delta\tau \tag{15}$$

in which, ρ indicates the evaporation rate and k stands for the iteration number. It is worth mentioning that evaporation is performed at every edge but pheromone is deposited only for the iteration-best or global-best tours, alternatively. However, it is also confined within the following lower and upper bounds in the proposed Min-Max ACO:

$$\tau_{\max} = 2\frac{W^{\min}}{L^{Best}} \tag{16}$$

$$\tau_{\min} = \frac{1}{3}\frac{W^{\min}}{L^{Best}} \tag{17}$$

In order to avoid algorithm stagnation in local optima, for every $\Delta k_{Stagnation}$ number of iterations that the algorithm experiences no improvement; the amount of pheromone at all the edges is re-initiated by $\tau_{reinitiate}$.

$$\tau_{reinitiate} = \frac{W^{\min}}{L^{Best}} \tag{18}$$

The probability of each node in the 2nd part of characteristic graph to be selected via the employed ACO is:

$$P_{ij} = \frac{\tau_{ij}\eta_{ij}^{\beta}}{\Sigma\tau_{ij}\eta_{ij}^{\beta}} \tag{19}$$

in which η_{ij} stands for attractiveness measure of the section (with index j) to be assigned to the i^{th} member group; that is inverse of its section area. This probability-based selection is activated when a random number generated in range [0,1] falls below a threshold q_0; otherwise the j^{th} state with maximal P_{ij} is strictly chosen:

$$j = \begin{cases} \arg.\max_{j}(P_{ij}) & if.rand > q_0 \\ with.probabilit y.P_{ij} & otherwise \end{cases} \tag{20}$$

An additional sizing intensification is also provided here by a similar approach to *branch and bound method* [18], BBM, to provide further improvement in the results of the ACO.

In the utilized method branches are grown toward lighter weight structures; i.e., neighbourhood of the section index for a current member group is searched increasing or decreasing its index by 1.

Consequently, an integrated framework is developed hybridizing HS, ACO and BBM in a suitable manner for

[Downloaded from ijce.iust.ac.ir on 2026-09-14]

the hyper optimization of the present engineering problem. The corresponding control parameters are employed as in Tables 1 and 2.

5. Numerical Examples

Two design types are considered in Table 3 for the present work; namely D1 as the hyper-optimized design for both sizing and loading pattern and the second design-type, D2, as merely sizing optimized under codified loading pattern of *Iranian Code of practice for Seismic Resistant Design of Buildings: standard-2800*, ICSRDB-05 [2]. In addition, four types of analyses are also considered as given in Table 4. The analysis types A1 and A2 denote static analyses under the optimized and code-specific lateral loads, respectively. A3 indicates the modal analysis using ICSRDB-05 spectrum and A4 denotes time-history analysis using acceleration records of the earthquakes given in Table 5. The spectral matching interval in the ICSRDB-05 scaling procedure is taken as $[0.2T_{Struct}, 1.5T_{Struct}]$ where T_{Struct} is the structures' fundamental period.

The design spectrum is formed for soil type III in the highest seismic hazard zone-4 due to ICSRDB-05. Figure 1 demonstrates the normalized spectrum evaluated for the corresponding parameters given in Table 6. Such a normalized spectral parameter, B, should be multiplied by the regional factor A, the importance factor I and the structural behaviour factor R to reveal the final spectral values for design. The base-shear is thus given by ICSRDB-05 as:

$$V = \frac{B.I.A}{R}W \tag{21}$$

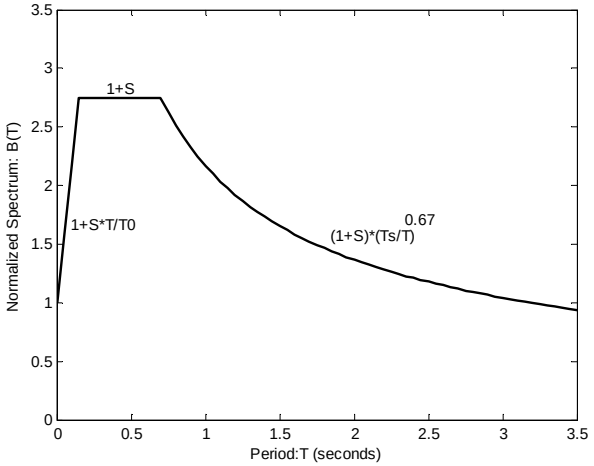

Fig. 1 The employed normalized design Spectrum due to Iranian Standard-2800[2]

where W is the total floors' weight computed by dead plus 20% live floor loads as recommended by ICSRDB-05. In all the examples AISC-ASD89 requirements are also considered for steel design of structural members using wide-flange IPB sections. The material properties of steel are taken the elasticity modulus of $200\,GPa$ with the yielding strength of $235\,MPa$.

Table 1 Control parameters for the utilized Harmony Search

HMS	BW	HMCR	PAR
30	0.5	0.90	0.15

Table 2 Control parameters for the utilized Min-Max ACO

Number of Ants	q_0	ρ	β	$\Delta k_{Stagnation}$
15	0.90	0.10	0.2	15

Table 3 Description of the employed design types

Design ID	D1	D2
Description	Both load-pattern and sizing optimized simultaneously	Sizing optimized under the code-based load-pattern

Table 4 Description of the employed analysis types

Analysis ID	A1	A2	A3	A4
Description	Static analysis under the optimized load-pattern	Static analysis under the code-based load-pattern	Modal analysis under code-based spectrum	Time-history analysis

Table 5 List of earthquakes used for time-history analyses after spectral scaling

Earthquake record ID	Duzce-1999	Imperial-1979	Kobe-1995	Tabas-1978	Mexico-1980	Northridge-1994	LomaPrieta-1989
PGA(g)	0.822	0.602	0.821	0.852	0.621	0.828	0.512
Epicentral distance (km)	17.6	3.8	0.6	3.0	34.8	6.1	13.0

Table 6 The employed factors for design spectrum according to the Iranian Standard-2800

S	T_0(s)	T_s(s)	A(g)	I	R
1.75	0.15	0.70	0.35	1	7

[Downloaded from ijce.iust.ac.ir on 2026-09-14]

Example 1: 10-Storey Moment Frame

A 2-bay 10-storey steel frame is considered here with storey-height of 3*m* bay-length of 5*m* in the longitude direction of Figure 2 and 4*m* in the transverse direction. Dead and live loads in the floor levels are taken $600 daN/m^2$ and $200 daN/m^2$, respectively; except for the roof live load that is $150 daN/m^2$. The member groups are taken symmetric as depicted in Figure 2. Both member cross-sections and lateral loading pattern (height-wise distribution of base-shear) is optimized in this example revealing design D1. Sample convergence curve of sizing optimization is shown in Figure 3 to insure proper trend of getting close to the optimal design as a result of balance between intensification and diversification in meta-heuristics [19-21]. In this example the elitist fitness has grown up rapidly in the early iterations and then has remained stable up to the iteration 200 when the result is announced as the optimal design.

As depicted in Figure 4, the optimized pattern of D1 is found different from the code-specific pattern by ICSRDB-05.

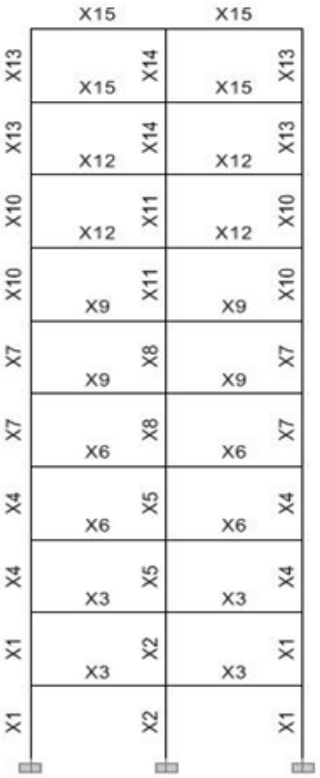

Fig. 2 Member groups for the first example

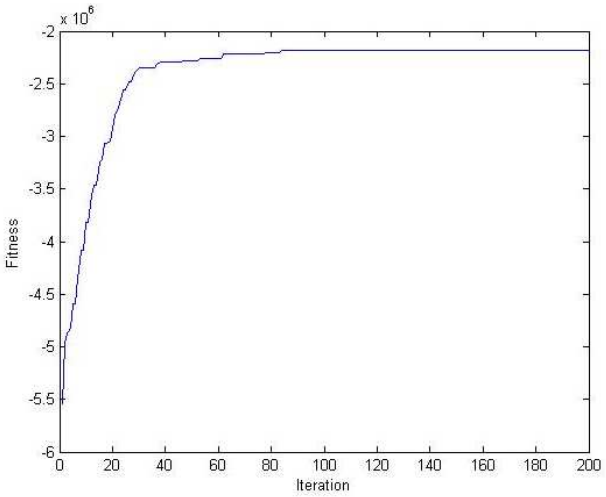

Fig. 3 Optimization convergence history for the 10-storey frame

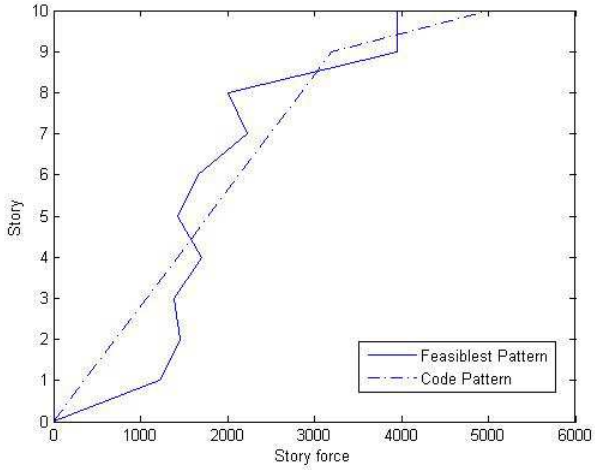

Fig. 4 Optimized vs. code-based distribution of base-shear (*daN*) in the 10-storey example

The achieved D1 pattern reveals more uniform load distribution in the middle floors and less in the upper ones with respect to the ICSRDB-05 code as a prototype for designing the frame. Note that this final design is the fittest during the optimization picked from those models which satisfy all the problem constraints. The frame sizing under ICSRDB-05 load pattern is also optimized to obtain its D2-type design using sections in Table 7 and 8. Table 9 demonstrates the base shear and its distribution patterns in this example where the structure's fundamental period is 1.026s.

Table 7 The Section-list used for beams in the optimal design

IPB10	IPB12	IPB14	IPB16	IPB18	IPB20	IPB22	IPB24	IPB26	IPB28	IPB30	IPB32	IPB34	IPB36	IPB40

Table 8 The Section-list used for columns in the optimal design

IPB10	IPB14	IPB18	IPB22	IPB26	IPB30	IPB34	IPB40	2IPB 10	2IPB 14	2IPB 18	2IPB 22	2IPB 26	2IPB 30

[Downloaded from ijce.iust.ac.ir on 2026-09-14]

Table 9 The base shear distributed as equivalent lateral forces for Designs D1 and D2 of the 10-storey example

Storey	D1 Forces (ton)	D2 Forces (ton)
1	1.37	0.39
2	1.63	0.79
3	1.54	1.18
4	1.89	1.58
5	1.58	1.97
6	1.85	2.37
7	2.47	2.76
8	2.21	3.16
9	4.39	3.55
10	4.37	5.55
Base Shear	23.30	23.30

The frame displacement response is monitored at the floor levels and normalized to its code-based limit for comparison purposes. According to Figure 5, the storey displacement responses in design D1 (both load pattern and sizing optimized) has get closer to its constraint limit in a more uniform manner with respect to the design D2 (sizing under code-based pattern). The fact is evaluated by several analysis types including A3 that reveals higher optimality under pattern-optimized loading than the code-based sizing design regarding Table 10. In addition, Figure 6 shows more uniform drift response in the proposed loading pattern with respect to code-based pattern. Note that more inter-storey drifts' uniformity means more participation of the entire structural elements in undertaking the seismic excitation effects and leads to more efficient or better seismic performance according to the current literature [4].

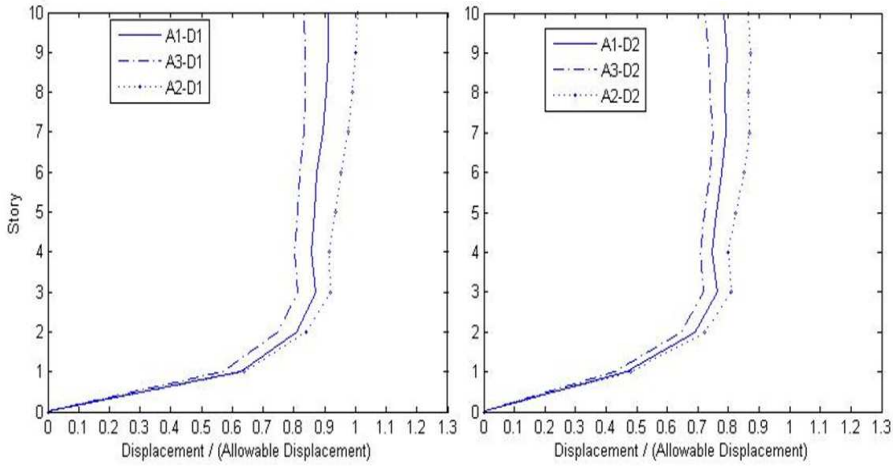

(a) (b)

Fig. 5 Displacement response of the 10-storey frame designs a) D1 and b) D2 by various analyses

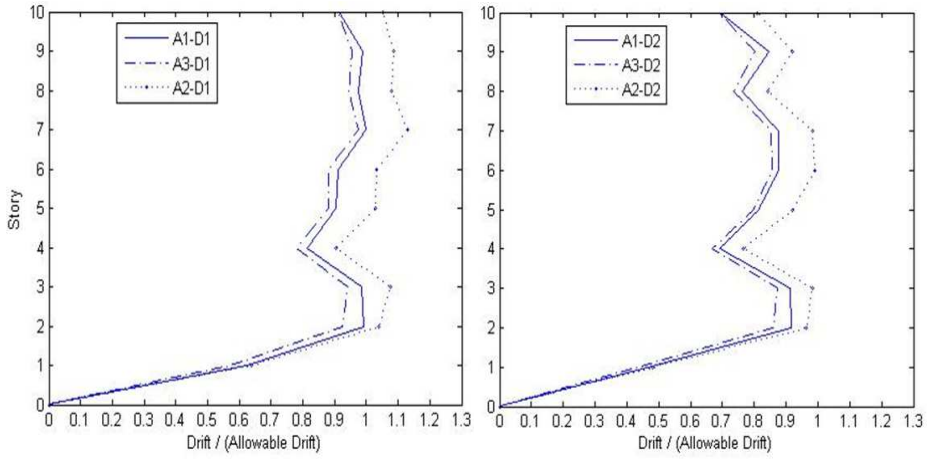

(a) (b)

Fig. 6 Drift response of the 10-storey frame designs a) D1 and b) D2 evaluated by various analyses

[Downloaded from ijce.iust.ac.ir on 2026-09-14]

Table 10 Comparison of various designs and analyses results in the 10-storey example

Example	Design ID	Optimized/maximal structural weight (%)	Storey of the 1st Failure identified by analysis A3	Storey of the 1st Failure identified by analysis A4
10-storey	D1	42	12	12
10-storey	D2	49	2	2

Location of the first column failure during earthquake in different designs is the next issue studied in the present research. It is desired to occur in less important stories for the overall structural stability; that is the upper stories rather than the lower columns which undergo more forces [22].

According to Table 10 the optimal structural weight in D1 design is 42% of a benchmark maximal weight slightly less than D2 (49%). However, their behaviours under earthquakes are quite different. The most critical column in the D1 designed model appears in the uppermost storey under both modal and time-history dynamic analyses A3 and A4, but such a failure starts in the 2nd storey for the D2 size-designed model under the ICSRDB-05 regulations. It confirms the result of Figure 7 in superiority of the proposed optimized pattern over traditional code-based pattern in viewpoint of progressive collapse prevention.

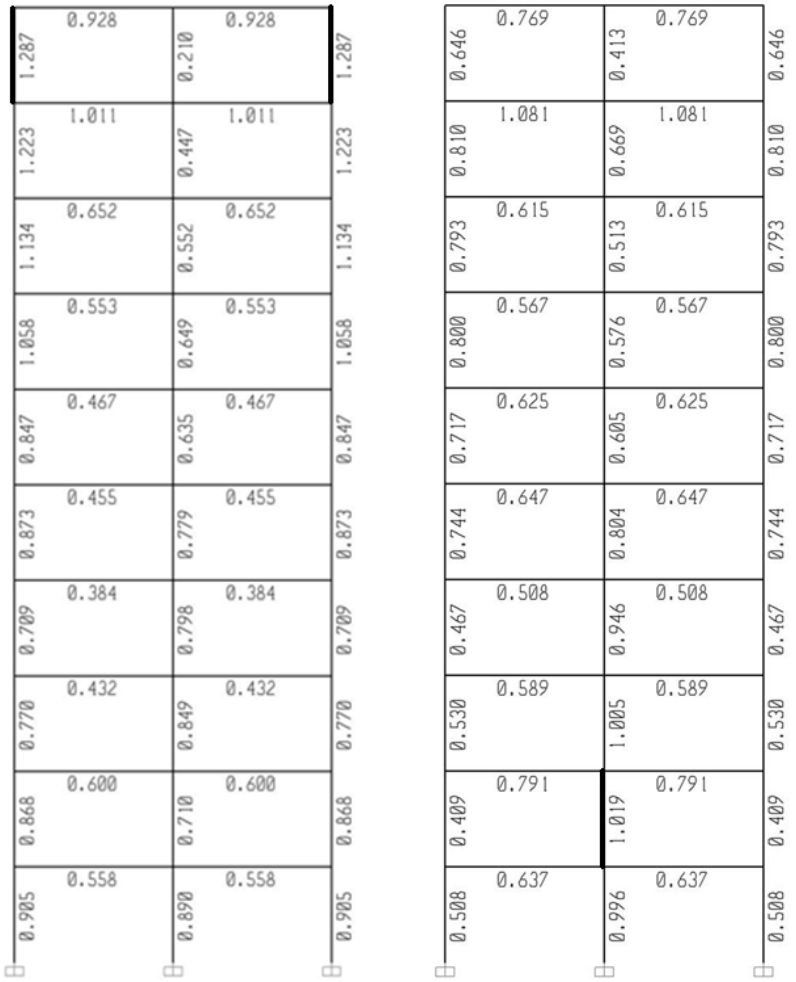

(a) (b)

Fig. 7 Critical stress ratios and location of failure-start evaluated by analysis A4 using the scaled records in the 10-storey example for design-types a) D1 and b) D2

Example 2: 15-Storey Moment Frame

The second example is a 2-bay 15-storey with 8 beam groups and 16 column groups demonstrated in Figure 8. The storey-height, bay-length and floor distributed loads are taken the same as previous example; while the number of stories is different in order to study its effect on the results. Convergence history of the fittest feasible design in Figure 9 again shows good algorithmic stability and efficiency to insure sufficient effort has consumed before announcing the optimal design. However, greater number of iterations is required for this taller building than previous example due to its higher cardinality of the search space. Hence, the elitist fitness became stable after 270 iterations up to 500. The control parameter HMS is taken 50 for this example.

[Downloaded from ijce.iust.ac.ir on 2026-09-14]

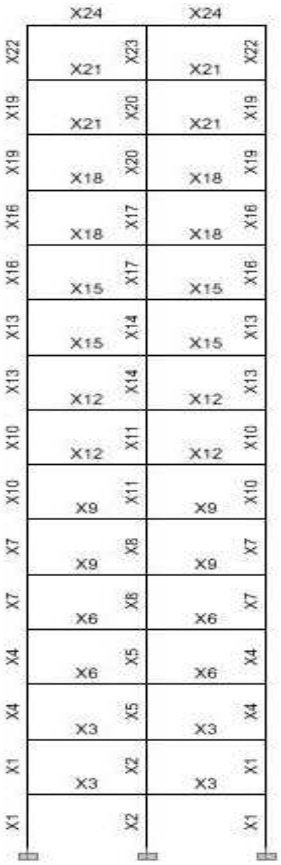

Fig. 8 Member grouping for the 15-Storey example

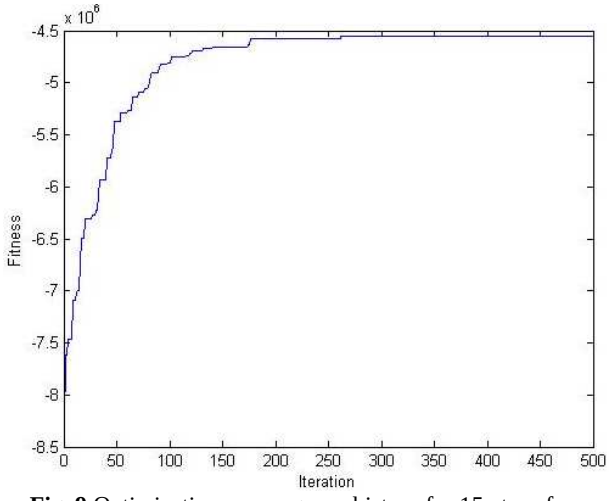

Fig. 9 Optimization convergence history for 15-story frame

Codified base shear and its distribution patterns in this example are given in Table 11 where the structure's fundamental period is 1.39s.

Table 11 The base shear distributed as equivalent lateral forces for Designs D1 and D2 of the 15-storey example

Storey	D1 Forces (ton)	D2 Forces (ton)
1	0.40	0.23
2	1.14	0.47
3	1.56	0.70
4	1.83	0.93
5	1.83	1.17
6	1.83	1.40
7	1.78	1.64
8	1.93	1.87
9	1.75	2.10
10	2.03	2.34
11	1.98	2.57
12	2.22	2.80
13	3.04	3.04
14	3.36	3.27
15	4.31	6.47

According to Figure 10 the optimal loading pattern as a result of D1 design for 15-storey frame shows similar trend to the D1 design of 10-storey example but in smoother manner; that is a rather more uniform distribution of base-shear as lateral loads in the middle part of the structure triangularly while increased near the roof level. In another word, the base-shear height-wise distribution pattern has shifted from upper stories to some mid-height lower stories in the optimal D1 design with respect to ICSRDB-05. It is expected to provide more stiffness and strength in the lower storey columns with respect to the upper ones under the code-based design pattern. Such a prediction is further confirmed by time-history analyses under several different earthquake records. As given by modal analysis, A3, in Table 12 the most critical column to fail first is identified at the 15th storey of this frame. Time history (A4) analyses under several scaled earthquake records have led to almost similar results (Table 13); just for two records out of 7 the critical columns are located at the 13th storey while it occurred at 15th storey for the D1 designed model of this example. In contrary, for the D2 model column failure started at the lowermost critical storey (1st) according to both spectral and time-history (A3 and A4) analyses.

Table 12 Comparison of various designs and analyses results in the 15-storey example

Example	Design ID	Optimized/maximal structural weight (%)	Storey of the 1st Failure identified by analysis A3
15-storey	D1	55	15
15-storey	D2	58	1

Table 13 Location of the 1st failure occurrence for design D1 of the 15-storey frame evaluated by time-history analyses using various earthquake records

Earthquake record ID	Duzce-1999	Imperial-1979	Kobe-1995	Tabas-1978	Mexico-1980	Northridge-1994	LomaPrieta-1989
Storey in which columns' failure starts	15	13	15	13	15	15	15

[Downloaded from ijce.iust.ac.ir on 2026-09-14]

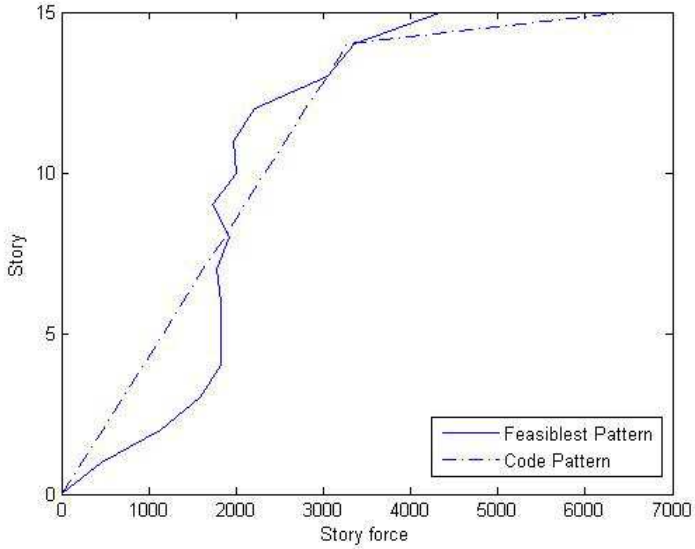

Fig. 10 Optimized vs code-based distribution of base-shear (*daN*) in the 15-storey frame

Normalized displacement and drift response at the storey-levels of the D1 and D2 designed 15-storey models are depicted in Figures 11 and 12, respectively. The drift responses for optimal design D1 under A1 analysis are obtained similar to A3 but different from the result of A2 analysis. The same is observed for the displacement response among the building height. Such conformity of the optimized lateral load pattern with the spectral design confirms true performance of the employed hyper-optimization algorithm in evaluating the fitness via spectral analysis.

The standard deviation of inter-storey drift response i.e.; 0.122 for D1 is less than 0.126 for D2 design. As evident from Figure 12, in the design D2 the greatest drift has undesirably taken place at the lower stories while optimizing load pattern in the D1 design has led it to locate at upper stories. The design-type D1 is thus superior with respect to design D2 regarding not only uniformity of drift responses but also preference of critical column location in preventing progressive collapse of the frame.

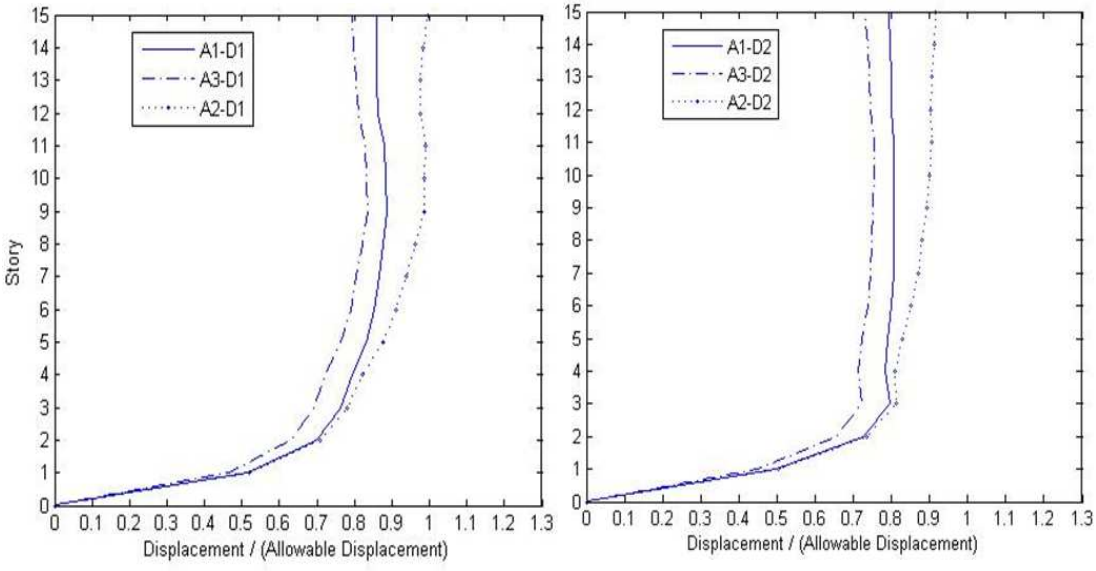

(a) (b)

Fig. 11 Displacement response of the 15-storey frame designs a) D1 and b) D2 evaluated by various analyses

[Downloaded from ijce.iust.ac.ir on 2026-09-14]

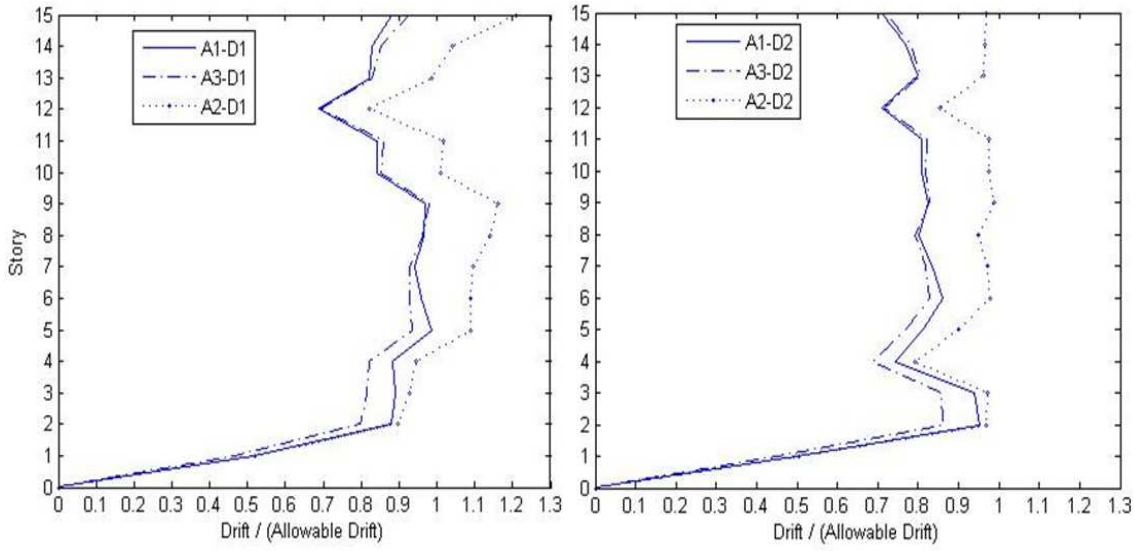

(a) (b)

Fig. 12 Drift response of the 15-storey frame designs a) D1 and b) D2 evaluated by various analyses

6. Conclusion

The present work revealed a design modification to improve behavior of steel moment frames under seismic excitations. Common descriptive codes offer an upper triangular-like pattern of base-shear distribution as equivalent lateral loads to be employed in allowable stress design procedure instead of complicated trial and error designs via dynamic time-history analyses.

In order to verify and upgrade suitability of such a design procedure, the optimal pattern of base-shear distribution has been searched simultaneously together with the corresponding optimal sizing of structural members. A two-fold optimization problem is then formulated using both discrete cross-section numbers and continuous distribution factors. Suitable search algorithms are picked up for each part of optimization considering the search space cardinality for such a complex problem; they are harmony search, ant colony and branch & bound methods hybridized in the present integrated optimization framework. Proposed definition of fitness function has also taken into account not only minimal structural weight but also both penalized constraint violations due to the design code and remunerating guided location of first plastic hinge formation among the frame height.

Treating a number of examples, the proposed algorithm revealed new patterns of equivalent lateral design loads similar to each other but different from traditional code-based pattern. It includes uniform distribution of base-shear over the mid-height stories which vanishes near the base and almost linearly increases near the top level.

As another goal in the current study guided failure sequence by design variation through different design-load patterns were investigated. It is observed via treated examples that the traditional code-based design may undesirably lead first stress concentration points to arise at the lower storey columns. As these columns have a critical role in resisting loads their failure can further lead to progressive collapse of the structure.

In the other hand, the proposed optimized pattern of lateral design-loads has been successful in guiding the critical location of such failure points to arise firstly at the higher storey levels, i.e.; less critical levels in overall stability of the frame. The achieved optimal designs were further verified by spectral and time-history analyses under scaled records of earthquakes with different frequency contents. The new optimal designs again stood superior with respect to those designed under the code-practice regarding the location of critically stressed storey-columns. Hence, it is concluded that the proposed method can decrease potential of progressive collapse during earthquakes.

Distribution of displacement and drift responses was another issue to be investigated here as a measure of safety according to the current literature. With respect to the code-based design, the proposed design procedure resulted in more uniform drifts among the frame height which means better participation of all structural elements in undergoing seismic drift demand and thus considered a safer design. It is worth mentioning that the optimal structural weight under the proposed optimal lateral load pattern obtained less than the result of sizing under the traditional code-practice.

In the view of treated examples and employed analyses, the proposed optimal lateral load pattern is offered for the equivalent static design procedure as it can lead to more economic or safer designs than current practice regarding uniformity of structural capacity distribution and guided failure sequence under seismic excitation.

References

[1] Uniform Building Code, International Conference of Building Officials, N.Y, 1997.

[2] Iranian Code of practice for Seismic Resistant Design of Buildings, Standard No.2800, 3rd ed, Building and Housing Research Center, 2005.

[3] Hosseini M, Motamedi M. A study on the distribution of

[Downloaded from ijce.iust.ac.ir on 2026-09-14]

lateral seismic forces in the height of R/C buildings by using nonlinear dynamic analysis, Proceedings of the 1st Conference of Iranian Society of Civil Engineers (ISCE), Tehran, Iran (Persian), 1999.

[4] Moghaddam H, Hajirasouliha I. A new approach for optimum design of structures under dynamic excitation, Asian Journal of Civil Engineering, 2004, Nos. 1-2, Vol. 5, pp. 69-84.

[5] Karami Mohammadi R, El Naggar MH, Moghaddam H. Optimum strength distribution for seismic resistant shear buildings, International Journal of Solids and Structures, 2004, Vol. 41, pp. 6597–6612.

[6] Kaveh A, Jahanshahi M, Khanzadi M. Plastic analysis of frames using Genetic and Ant Colony algorithms, Asian Journal of Civil Engineering (Building and Housing), 2008, No. 3, Vol. 9, pp. 229-249.

[7] Shahrouzi M, Rahemi AA. Effect of lateral loading patterns on seismic design of building frames, Proceedings of 4th National Congress on Iranian Code of Practice for Seismic Resistant Design of Buildings, Standard No.2800-2005, Building and Housing Research Center, Tehran, Iran (Persian), 2009.

[8] AISC-Allowable Stress Design and Plastic Design Specifications for Structural Steel Buildings, American Institute of Steel Construction: Chicago, IL, 1989.

[9] Lee KS, Geem ZW. A new meta-heuristic algorithm for continuous engineering optimization: harmony search theory and practice, Computer Methods in Applied Mechanics Engineering, 2005, Vol. 194, pp. 3902–3933.

[10] Geem ZW, Kim JH, Loganathan GV. A new heuristic optimization algorithm: harmony search, Simulation, 2001, No. 2, Vol. 76, pp. 60-68.

[11] Geem ZW. Music-Inspired Harmony Search Algorithm: Theory and Applications, 1st ed, Springer, 2009.

[12] Saka MP. Optimum design of steel sway frames to BS5950 using harmony search algorithm, Journal of Constructional Steel Research, 2009, No. 1, Vol. 65, pp. 36–43.

[13] Shahrouzi M, Rahemi AA. Utilization of harmony search for design of civil structures, Proceedings of 5th National Congress on Civil Engineering, Ferdowsi university of Mashhad, Mashhad, Iran (Persian), 2010.

[14] Moscato P. On evolution, search, optimization, genetic algorithms and martial arts: towards memetic algorithms, Tech. Rep. Caltech Concurrent Computation Program, Report. 826, California Institute of Technology, Pasadena, CA, 1989.

[15] Dorigo M, Colorni A. ManiezzoV. The Ant System: optimization by a colony of cooperating agents, IEEE Transactions on systems, Man and Cybernetics, 1996, No. 1, Vol. 26. pp. 1-13.

[16] Dorigo M. Ant Colony Optimization, M.I.T. press, 2004.

[17] Shahrouzi M. Pseudo-random directional search: a new heuristic for optimization, International Journal of Optimization in Civil Engineering, 2011, No. 2, Vol. 1, pp. 341-355.

[18] Burns SA. Recent Advances in Optimal Structural Design, University of Illinois at Urbana-Champaign, 2002.

[19] Kaveh A, Nasr H. Hybrid harmony search for conditional p-median problems, International Journal of Civil Engineering, 2012, No. 1, Vo. 10, pp. 32-36.

[20] Kaveh A, Nasrolahi A. A new probabilistic particle swarm optimization algorithm for size optimization of spatial truss structures, International Journal of Civil Engineering, 2014, No. 1, Vol. 12, pp. 1-13.

[21] Abbasi M, Markazi A.H.D. Optimal assignment of seismic vibration control actuators using genetic algorithm, International Journal of Civil Engineering, 2014, No. 1, Vol. 12, pp. 24-31.

[22] Bangash MYH, Bangash T. Explosion-Resistant Buildings, Design, Analysis, and Case Studies, Springer-Verlag, N.Y, 2006.

[Downloaded from ijce.iust.ac.ir on 2026-09-14]